Composition of the crust and upper-mantle in the Central Andes (19°30′S) inferred from P wave velocity and Poisson's ratio

C. Dorbath[a,b,*], F. Masson[c]

[a]*IRD, 213 rue La Fayette, 75480 Paris Cedex 10, France*
[b]*CNRS UMR 7516, Institut de Physique du Globe, 5 rue René Descartes, 67084 Strasbourg Cedex, France*
[c]*CNRS UMR 5573, LGTS, ISTEEM, Université Montpellier II, place Eugène Bataillon, 34095 Montpellier Cedex, France*

Abstract

The present-day crustal structure of the Andean chain results from deformation processes and magmatic activity since the onset of subduction. One line of investigation to resolve questions about the mechanism of crustal thickening is to get information about the composition of the crust and upper-mantle by imaging the structures in velocity and Poisson's ratio (or V_p/V_s). A high density seismic network was operated during six months in 1994 across the whole Andean chain. The P and S travel times of the best located local earthquakes, mainly situated in the subduction zone, have been inverted for V_p and V_p/V_s using Thurber's 3D iterative simultaneous inversion method. The resulting models, giving short-scale information about the crustal and upper-mantle composition, provide new limits on the respective involvement of crustal shortening and magmatism in the thickening of the Andean crust.

Beneath the Western Cordillera, the seismic properties are well explained by typical active volcanic arc processes, and the thickening of the crust is explained by magmatic addition. Conversely, beneath the Central Altiplano Basin and the Eastern Cordillera, our results preclude significant volume of magmatic addition from the mantle and reinforce crustal shortening as the main thickening process. Moreover, cratonic lower crust and subcontinental lithospheric upper-mantle are observed under the Eastern Cordillera up to 67°W, evidence of the underthrusting of the Brazilian craton, which drives the crustal shortening. Beneath the Central Altiplano Basin, a thin lithospheric mantle is observed above a well marked asthenospheric wedge which extends in depth below the western part of the Eastern Cordillera. Thus partial melt is observed in the shallow mantle west of the Western Cordillera up to the Brazilian craton. © 2000 Elsevier Science B.V. All rights reserved.

Keywords: Poisson's ratio; Andean chain; asthenospheric wedge

1. Introduction

In the last decades, a considerable body of information has been collected concerning the geological and geophysical structure of the Central Andes (Fig. 1). In particular, these data provide evidence of the extreme thickening of the Andean crust (e.g. James, 1971; Wigger et al., 1994; Scheuber and Giese, 1999) allowing investigation of the processes building the chain. The present day crustal structure results from deformation processes and magmatic activity since subduction began. Balanced cross-sections based on the geometry of near surface structures quantify the amount of horizontal shortening (Sheffels, 1990; Schmitz, 1994; Baby et al., 1997); they show that a

* Corresponding author. Institut de Physique du Globe, 5 rue Rene Descartes, 67084 Strasbourg Cedex, France. Tel.: +33-88-41-63-96.

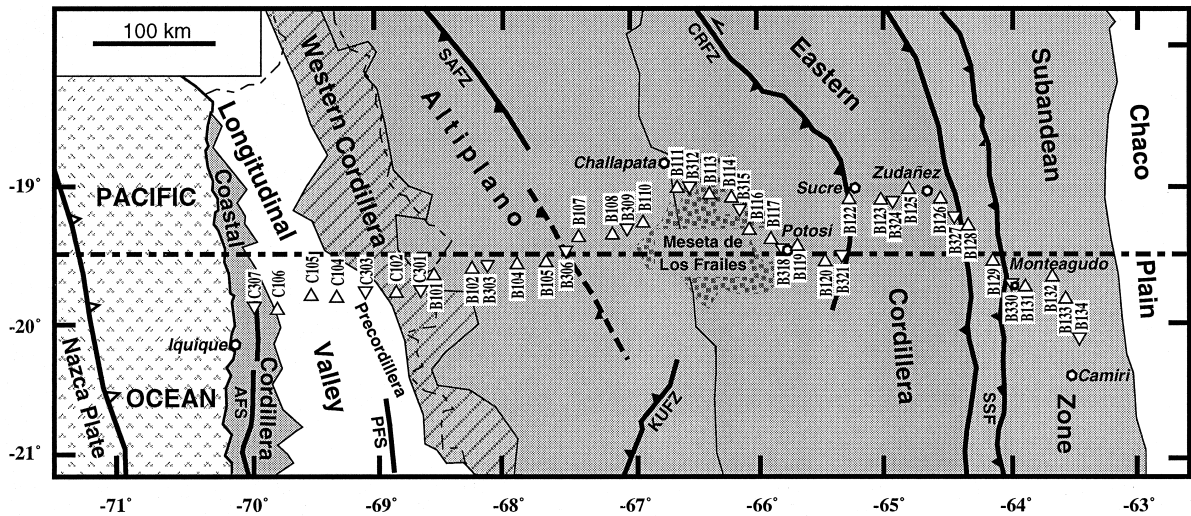*E-mail address:* cath@mapu.u-strasbg.fr (C. Dorbath).

Fig. 1. Distribution of the temporary stations used for the local earthquake tomography. The triangles indicate the location of the stations (triangle up: 1C station, triangle down: 3C station), the dashed line indicates the location of the cross-sections presented on the Figs. 3 and 4. The present day structure of the chain, along an east–west transverse, is characterized by different north–south morphological units which are, from the west to the east, the Coastal Cordillera, the Longitudinal Valley, the Precordillera, the Western Cordillera, the Altiplano, the Eastern Cordillera and the Subandean Zone. These morphological units are not exactly superposed to the geological structures. The Western Cordillera is a part of the Altiplano crowned by volcanoes. From the coast to the Chaco plain, the Andean chain has here its largest width (about 700 km). The mean elevation is near 4000 m in the Altiplano and the Eastern Cordillera and can reach locally 5000 m in the Western Cordillera and in the Meseta de los Frailes, a late Cenozoic volcanic field.

significant amount of the crustal volume must be explained by sources other than crustal shortening. The main candidate processes to explain the excess material in the deeper crust are underplating of tectonically eroded material of the continental margin and magmatic addition at the basis of the crust (Schmitz et al., 1997; Myers et al., 1998; Rochat et al., 1999), the contribution of each process depending on the morphological unit considered.

One line of investigation to resolve the question of the crustal thickening is to get information about the composition of the crust and upper-mantle by imaging the structures in velocity and Poisson's ratio (or, equivalently, V_p/V_s). While the non uniqueness of the relationship between P wave velocity and material composition is well known, V_p/V_s ratio measurements provide constraints on fluid pore pressure, fabric and temperature conditions (Christensen, 1996; Musacchio et al., 1997).

Several recent geophysical studies have investigated this question. Zandt et al. (1996) modelled broadband waveforms for paths mainly crossing the Altiplano and found a mean crustal Poisson's ratio σ

of 0.25. From this value, they deduce a felsic crust which precludes magmatic addition and reinforces they hypothesis of crustal shortening to explain the great thickness of the Altiplano crust. Just refining this work, Swenson et al. (2000) find a north–south variation in the structure of the Altiplano, with a mean P wave velocity lower and a σ in the crust slightly higher south of 20°S.

However, from gravity studies, Schmitz et al. (1997) suggest partial melt beneath the Western Cordillera and the western part of the Altiplano at 21–23°S. Model calculations of the gravity field based on the crustal structure deduced from seismic refraction profiles (Wigger et al., 1994) lead to an overcompensation of the observed Bouguer anomaly using classical velocity–density relationships. Schmitz et al. (1997) explain the abnormal observed velocity–density relationship by the presence of partially molten rocks at depth. Moreover, Schmitz et al. (1997) consider that the expected value for σ, in case of a "normal" composition of the crust down to 45–50 km depth above a partially molten lower crust, is in good agreement with the mean

value of 0.25 obtained by Zandt et al. (1996). More recently, Myers et al. (1998) developed a lithospheric-scale model at 20°S based on tomographic images of velocity and attenuation for P and S waves. They focus their discussion on the shallow mantle, and find an average velocity and Q significantly higher than in most mantle wedge environments, likely the result of a compressional "back arc" setting in the Andes. They observe lithospheric mantle under the Altiplano, the Eastern Cordillera and the sub-Andes, and propose different mechanisms of volcanism under the two Cordilleras: arc volcanism in the Western Cordillera and upward migration of mantle wedge asthenosphere following the removal of thickened lithosphere for the Altiplano/Eastern Cordillera border region. Beaumont et al. (1999), using the seismological data of temporary networks installed across the Andes between 1990 and 1995, studied the amplitude of the Lg phase. They find a strong attenuation in the crust of the whole Altiplano. Their study of the frequency-dependence of Q indicates that the attenuation is due more to scattering by small scale heterogeneities than to a high percentage ($>1\%$) of partial melting involving a large part of the crust.

Three-dimensional models of P wave velocity and P to S velocity ratio were obtained by Graeber and Asch (1999) near 23°S from the Pacific coast to the Western Cordillera (PISCO '94 experiment). They show anomalously high V_p/V_s ratios in the deeper part of the forearc indicative of a hydrated mantle wedge. A zone of high attenuation Q_p high V_p/V_s ratios and low velocity beneath the magmatic arc indicates partially molten rocks from a depth of 20 km down to the asthenospheric wedge.

The Myers et al. (1998) results are based on data from mantle earthquakes recorded by two portable seismic cross-shaped networks. One of them, the BANJO array, was an east–west array of 16 broad-band stations traversing the Andes between 19°S and 20°S, with a station spacing of about 40 km. At the same time, a French Lithoscope experiment was developed along the same east–west profile. 55 short-period portable stations (41 vertical and 14 three component stations) were operated during six months across the Andean chain (Fig. 1). This higher density seismic network (station spacing about 15 km) recorded distant earthquakes and local events. P-teleseismic delay times were used to perform a tomographic

inversion in order to examine the lithosphere and the mantle down to 600 km, and the subducted slab (Dorbath and Paul, 1996; Dorbath, 1997). Masson et al. (2000) performed the inversion of P travel times of local earthquakes located mainly in the subduction zone, and described the Andean chain in term of P-wave velocities. In this study we will further interpret the results of the local earthquake inversion, examining spatial variation of Poisson's ratio σ beneath the Andes. In particular, the narrow station spacing allows us to image the crust in detail, and a direct comparison of our results with similar results obtained by Myers et al. (1998) in the shallow mantle is possible. A complete description of the experiment and of the geological setting has been done in the previous papers (Dorbath and Paul, 1996; Dorbath, 1997; Masson et al., 2000), and will not be repeated in this paper.

2. Data and method

We briefly outline the data selection fully described in the Masson et al. (2000) paper. As the network was quasi linear, we included offline stations when computing the location of the local earthquakes recorded at the temporary stations. Thus we used 68 stations for the initial hypocentral, determinations, including the Bolivian permanent stations and the Antofagasta (Chile) array (Fig. 2). Great attention was paid in the S arrival time selection. The use of 19 three component stations with different azimuths and epicentral distances strongly reduces the risk of mis-identification of S waves. Moreover, the seismograms are generally simple with impulsive P and S arrivals (see Myers et al., 1998, for an example). A discussion about phases picking and a study of P travel time residuals is included in Masson et al. (2000) paper. Among the 280 local earthquakes recorded, we kept the 163 very best located earthquakes (Fig. 2) providing 2704 P and 748 S arrival times.

The local arrival times were simultaneously inverted for hypocenters and 3D velocity structure using *simulps12* code (Evans et al., 1994) adapted from the method developed by Thurber (1983). Graeber and Asch (1999) chose the same routine to perform the 3D inversion of the data collected during the PISCO'94 experiment for a 4 by 4° area. Initially,
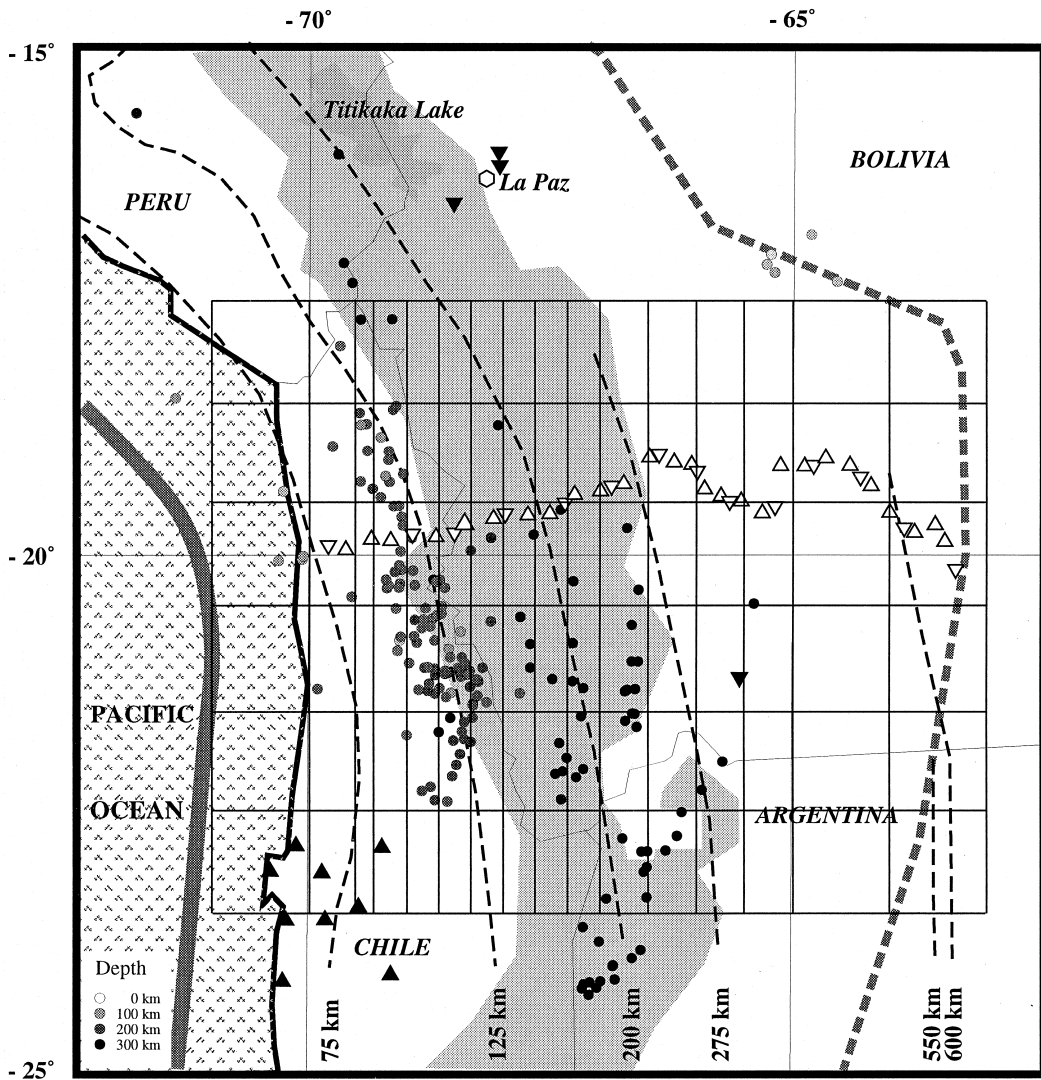
Fig. 2. Distribution of events used for the local earthquake tomography and of stations used for hypocentral location (from Masson et al., 2000). The shaded circles show the relocated epicenters after the inversion, the darker the deeper. The triangles indicate the location of the stations (white up: 1 component temporary station — white down: 3 component temporary station — black up: Chilean permanent station of the Antofagasta array — black down: Bolivian permanent station). The shaded area represents the Altiplano (Peru — Bolivia) and Puna (Argentina). The bold dotted line indicates the limit of the Subandean zone. The thin dotted lines indicate the depth of the subducted slab (Kirby et al., 1995). The geographical location of the inversion grid (without peripherical nodes) is reported.

the approximate ray tracing algorithm used in the Thurber's method was developed to inverse arrival times of local events, with a maximum station event distance of about 50 km. The use of this method is questionable when the station–event distance is larger. In this study, the maximum station event distance taken into account is 550 km. We have

performed a synthetic test in order to check the reliability of the method when it is applied to our large scale display. For each event used in the inversion, a set of theoretical travel times through a 1D model has been computed. Introducing these travel times as input of the local earthquake tomography, the initial tabular velocity model is retrieved, with a mean error

per layer of about 1%. This error is much smaller than the average standard deviation per layer obtained during the inversion of the real data (Masson et al., 2000; Table 1). Therefore, Thurber's method seems to be applicable for our specific problem. This result is due to the fact that all the parameters of the inversion increase simultaneously the depth of the events, the station event distance, the mean value of the residuals and the chosen size of the cells used during the inversion. There is a scaling factor and the ratio of the residual travel time to the ray tracing error remains constant.

Our purpose being to obtain Poisson's ratio values, we preferred to calculate V_p and V_p/V_s models rather than V_p and V_s models. In cases where S data are less numerous and of poorer quality than P data, V_s models are less resolved than V_p models, and the simple division of the models gives V_p/V_s values difficult to interpret (Eberhart-Phillips and Michael, 1998). Following Foulger et al. (1995), we produced first a detailed V_p model using a constant V_p/V_s ratio, 1.74, obtained by a Wadati diagram of our data. Thus we permit the use of S travel times in event location steps but did not allow V_p/V_s to vary. The detailed model of V_p completed, we proceeded to the full inversion for V_p and V_p/V_s starting with the detailed V_p model, a uniform V_p/V_s model, and allowing inversion for both. At that step, the V_p model changes very little. Compared with the V_p/V_s model obtained directly by a simultaneous inversion with V_p, our solution is very close but smoother.

The initial V_p model was the same as in Masson et al. (2000). Damping values were chosen with trade-off curves of data variance against solution variance for both variables. The parametrization of the final model was slightly different from Masson et al. (2000) study. It consisted in 7 grid layers from the surface down to 220 km. The horizontal grids were centered on $19°30'$S, with a 1° grid spacing in latitude. In longitude, the grid spacing was not regular, in order to account for ray paths density; it was half a degree from 65°W to 67°W and third of a degree from 67°W to 70°W, where the great majority of earthquakes occurred (Figs. 2 and 3). Later on, we will present a cross-section through the models below the seismic array, at $19°30'$S, where the resolution is the highest. The values of the diagonal elements of the resolution matrix are presented on the Fig. 3

interpollated between the nodes, together with the number of hundred of rays contributing to the resolution of each node. With these parameters, the final model has variance reduction of 88% for V_p and 73% for V_p/V_s from the initial coarse model.

3. Results and discussion

We present in Fig. 4 the cross-sections through the final models. As V_p/V_s ratios have initial values independent of the depth, the image of the vertical cross-section is the same in true V_p/V_s value or in perturbation of V_p/V_s (Fig. 2c). This is obviously not the case for the V_p cross-section because the initial model of V_p increases with depth. Thus, in order to make the results more readable, we chose to present in this paper V_p (Fig. 2a) as well as the V_p perturbations with respect to the initial model (Fig. 2b). The main faults and the limits of the tectonic units (Masson et al., 2000) are shown on the cross-sections, as well as the Moho discontinuity defined as the steepest velocity gradient on the V_p model and the top of the subducted Nazca plate defined by the Wadati Benioff zone (Kirby et al., 1995). We focus our discussion on the part of the model situated between 67 and 69°W, which is the best resolved, and which is also a key region for understanding the Andean building processes.

3.1. The crust

In the upper-crust, a good agreement between the velocity model and the geological structures is observed. Generally, high velocities coincide with zones where basement is present near the surface while low velocity zones are clearly associated with the presence of very thick sedimentary basins or volcanic material. The main fault systems are closely related to the limits of the velocity zones. They define large domains and extend to greater depth, dipping to the west as suggested by isovelocity lines (Masson et al., 2000).

A decrease or increase of both V_p and V_p/V_s is observed in some places, when in other places these seismic parameters do not vary together. Moreover, there are domains where the relative variations of V_p and V_p/V_s are not the same in the upper and in the lower crust. When both σ and V_p increase or decrease
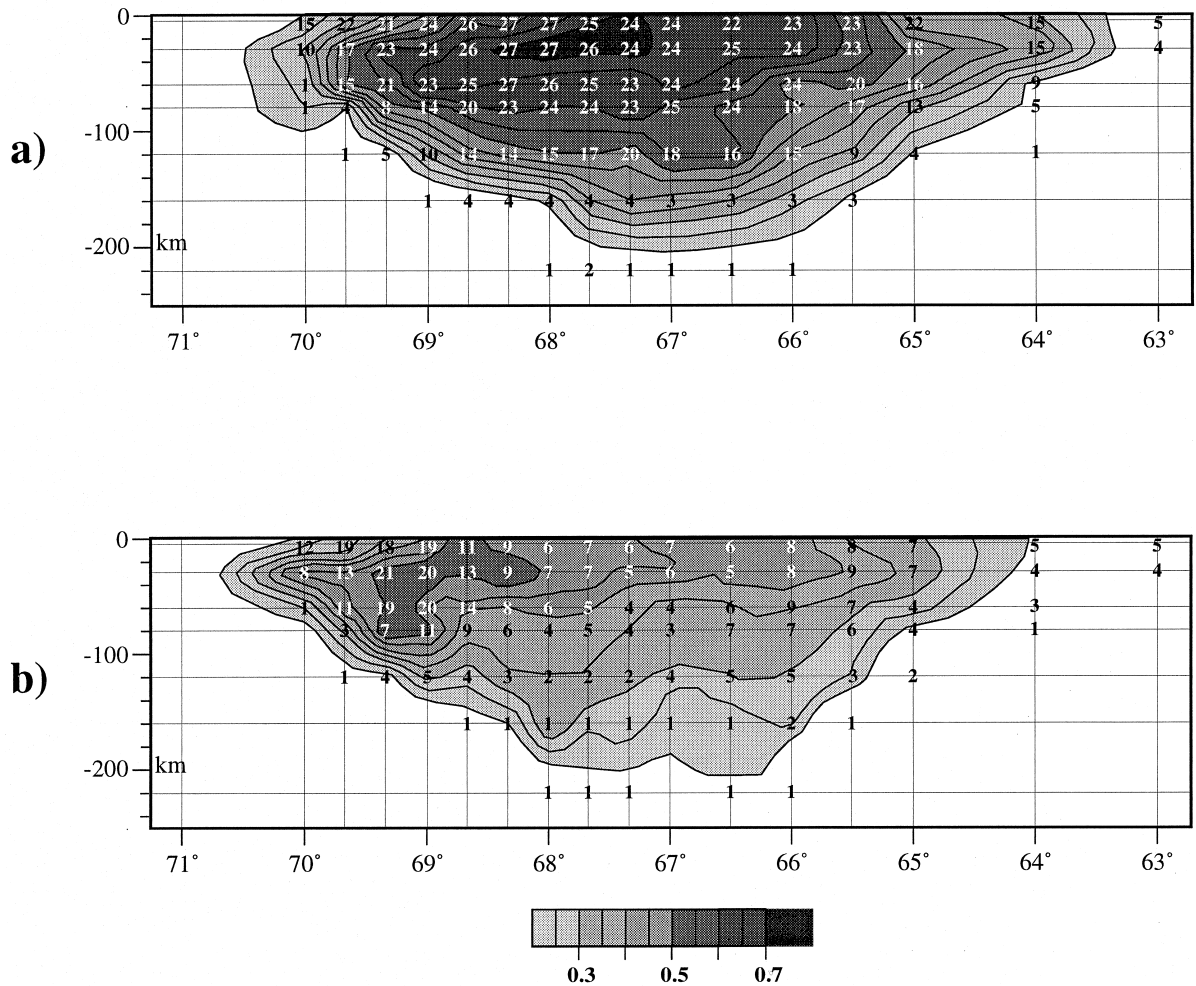
Fig. 3. Cross-sections at 19°30′S through the values of the diagonal elements of the resolution matrix for: (a) the V_p and (b) the V_p/V_s models. The darkest zones are the best resolved in the inversion. The numbers on the grid nodes represent the hundred of rays crossing in their vicinity and contributing to their resolution.

together, the composition of the material has to be considered first. On the other hand, high pore pressure results in a greater decrease of V_s than V_p, hence a high V_p/V_s ratio. Thus we will describe separately the models in the upper and lower crust.

3.2. The upper-crust (0–30 km)

In the upper crust, high σ and high V_p are observed in three zones: beneath the Precordillera, at the limit between the Western Cordillera and the Central Altiplano Basin (SAFZ), and beneath the Eastern

Cordillera west of CRFZ. However, the amplitude and the size of the variations are more marked for σ. These three zones of simultaneous high V_p and high σ correspond to zones of shallow Precambrian rocks. Along the Precordillera, around C102, outcrops of Precambrian rocks have been observed (Basei et al., 1996; Riquelme and Hérail, 1997). Around B105, Martinez et al. (1995) have proposed a westward dipping Precambrian block overthrusting the Central Altiplano Basin. Lastly, east of B117, Precambrian basement uplifted by imbricated thrusts has been suggested by Kley (1996). Simultaneous high V_p and
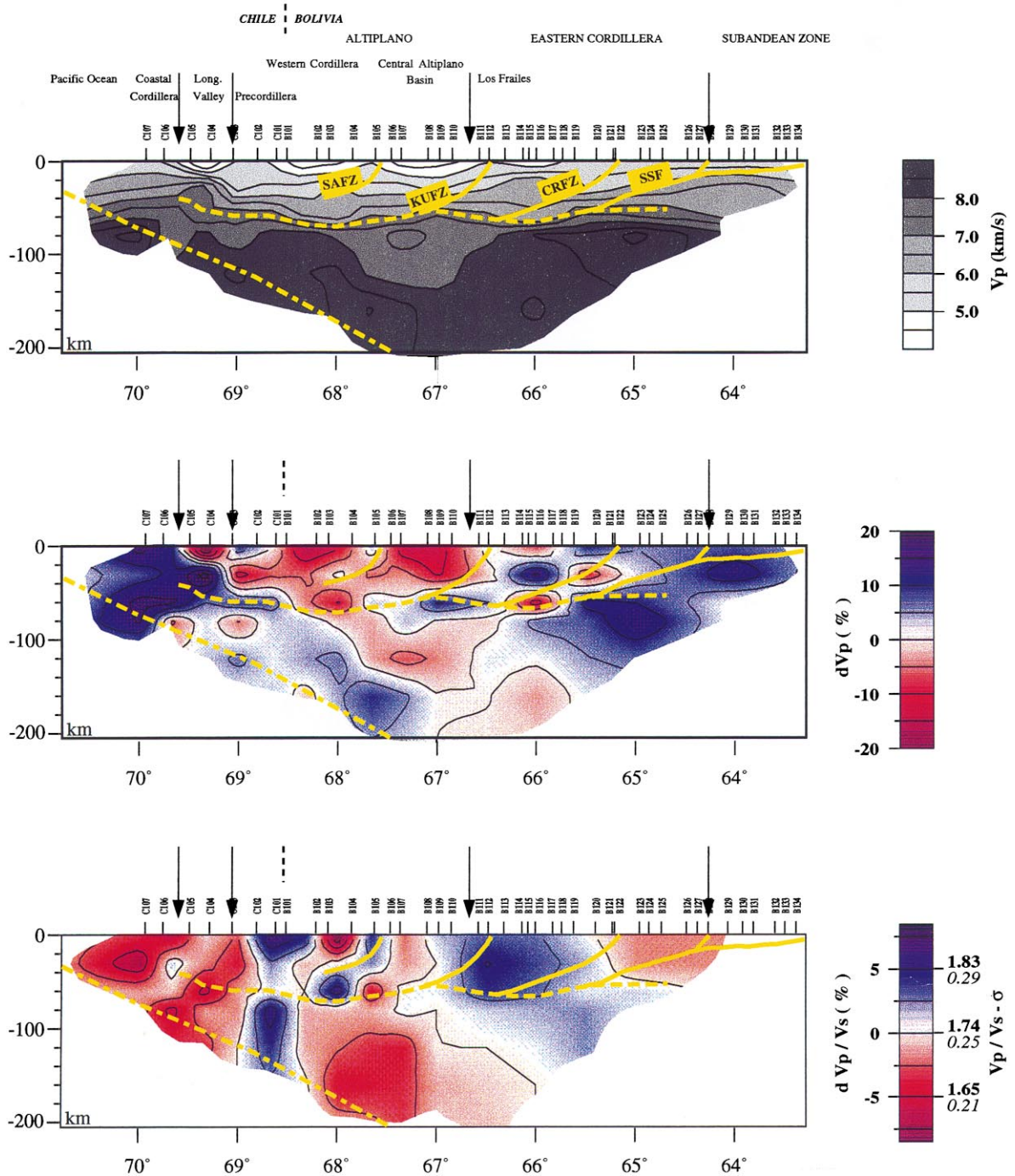
Fig. 4. Cross-sections at 19°30′S through: (a) the P-wave velocity model in km/s; (b) the P-wave velocity perturbation model in %; (c) the V_p/V_s model. The limits of the tectonical units are reported on each section, together with the main faults (thick yellow lines), the top of the subducting Nazca plate, and the Moho discontinuity (Masson et al., 2000). No vertical exageraction.

high σ imply a mafic composition (Musacchio et al., 1997). The Precambrian upper crust is estimated to have a felsic to intermediate composition, when lower crust is rather mafic (Zandt and Ammon, 1995). Thus, we suggest the origin of the uplifted Precambrian rocks is in the lower crust.

Inversely, low σ and low V_p are observed beneath the Longitudinal Valley, the Western Cordillera and the Central Altiplano Basin. In this case, the low σ zones are narrower than their associated low velocity zones. In the Longitudinal Valley, as in the Central Altiplano Basin, the low V_p anomaly is much more marked than V_p/V_s. The Altiplano basin contains thick sediment sequence (sandstones, shales and limestones (Pareja et al., 1978; Ardill et al., 1996)) underlain as expected, by low V_p and low σ. The presence of Neogene ignimbritic volcanism and of a moderate amount of sediment in the Longitudinal Valley (Scheuber et al., 1994; Pinto Linconir, 1999) can also explain our observations. It is more difficult to explain the observed narrow zone of very low σ associated with low V_p beneath the Western Cordillera. If the Western Cordillera is related to neogene volcanic material of the main volcanic arc as proposed by Backer and Francis (1978), higher V_p and higher σ should be expected. The observed low V_p and low σ may be due to the presence of a majority of acid volcanic rocks. The presence of ignimbrites widely distributed in the Cordillera seems not sufficient to explain the observation. An alternative explanation could be that there is only a thin layer of neogene volcanic material covering a thick Mesozoic and Cenozoic sediment sequence, and thus the Western Cordillera and the Altiplano Basin are similar sedimentary basins separated by uplifted Precambrian rocks. This speculation explains the apparent symmetry of both low V_p zone but not the differences in the low σ zones.

The eastern part of the Eastern Cordillera shows high σ and low V_p. It is centered below the silicic Los Frailes volcanic field. The anomalously high value of σ for acid rocks, also observed by Myers et al. (1998), could indicate the presence of high pore pressure in this region.

3.3. The lower-crust (30 km to Moho)

At greater depths, corresponding to the lower-crust,

the V_p and σ perturbations are generally smoother, but in some units the relation between them is the opposite of that observed in the upper crust. Beneath the Precordillera and the Western Cordillera, σ is higher while V_p is lower, this trend being much more marked below the Western Cordillera. A decrease of the average crustal velocity is observed from refraction studies by Wigger et al. (1994), with anomalously low velocities of 5.9–6.0 km/s in the deeper crust of the Western Cordillera at 21–23°S, 200 km south. A joint analysis of seismic and gravity data led Schmitz et al. (1997) to propose a model where the deeper Andean crust is strongly weakened by the presence of partially molten rocks beneath the arc and parts of the backarc. Therefore, beneath the arc, their model is supported by our results, the conjunction of low V_p and high σ suggesting partial melting (Schmitz et al., 1997).

Below the Central Altiplano Basin, low V_p values are associated with less pronounced low σ values down to the Moho depth. The combination of these seismic characteristics ($V_p = 6.0$ km/s, $\sigma = 0.25$), indicative of a felsic composition, is found by Zandt et al. (1996) in a study of the Altiplano crust for a much wider region. A felsic composition at such depth precludes significant volumes of magmatic addition from the mantle, and suggests crustal shortening as the main contribution to crustal thickening (Zandt et al., 1996). This conclusion is rejected by Schmitz et al. (1997) who proposed that this observed mean. Poisson's ratio for the whole thickness of the crust is in accordance to the value expected for a partially molten lower crust and a solid upper crust. Our results show that the V_p/V_s value is even lower in the lower crust indicating that the Zandt et al. (1996) interpretation is valid, but only for the Central Altiplano Basin. Magma addition, as proposed by Kono et al. (1989) or Zandt et al. (1996) south of 21°S is unlikely in the studied area.

In the western part of the Eastern Cordillera, up to CRFZ, both σ and V_p are rather high, which indicates a rather mafic composition expected for lower crustal rocks of cratons (Zandt and Ammon, 1995). From seismic refraction studies, Wigger et al. (1994) found a high velocity lower crustal layer extending from the sub-Andes to about the Altiplano/Eastern Cordillera boundary which is in the light of Myers et al. (1998), indicative of intermediate to mafic composition. The easternmost part of our V_p/V_s

model is not well resolved, nevertheless the high V_p are clearly associated with the Brazilian shield. Then, the seismic characteristics of the lower crust beneath the Eastern Cordillera, consistent with cratonic values, confirms that the western limit of the underthrusting of the Brazilian Shield is 67°W at this latitude, as postulated by Masson et al. (2000).

3.4. The mantle

The shallow mantle above the subduction zone, presents large regions with contrasted velocities. Beneath the Western Cordillera, we observe no V_p variation associated with a narrow vertical zone of significant increase of the V_p/V_s ratio. Beneath the Central Altiplano Basin we observe a large zone of low σ extending in depth under the western part of the Eastern Cordillera. The contrast attain maxima between 67 and 68°W below a 120 km depth down to the slab. In this region, we observe a less contrasted lower V_p only between 100 and 160 km depth, extending also in depth toward the east. On the other hand, a thin zone of high V_p is observed just below the Moho beneath the Central Altiplano Basin and the border of the Eastern Cordillera. The eastern part of the Eastern Cordillera is characterized by very high V_p and moderately high σ. The mantle is well resolved by the Myers et al. (1998) tomography, so we compare the studies without repeating the discussion already published in their paper.

Below the Western Cordillera, Myers et al. (1998) also find high σ values, when they observe localized V_p and V_s reduction. On both the northern (southern Peru) and southern (northern Chile) sides of our study area, low V_p and high σ are observed beneath the same structural unit (Cunningham et al., 1986, Graeber and Haberland, 1996). Taking into account laboratory experiments as well as subduction-related volcanic arc properties, the seismic properties observed can be explained by an extreme hydratation of the medium (Giese et al., 1999). Our results are compatible with this hypothesis, but we do not observe the localized low velocity anomalies that they interpret as pockets of partial melt.

Below the Altiplano, at 19°S, Myers et al. (1998) model a high V_p/normal V_p/V_s layer down to 125–150 km in the shallow mantle. We observe a similar anomaly, consistent with mantle lithosphere composi-

tion, but only in a thin layer at about the Moho depth. Below 100 km, the seismic properties that we find (lower V_p, very low σ) are characteristic of mantle asthenosphere. Similar seismic values are observed by Myers et al. (1998) at the boundary between the Altiplano and the Eastern Cordillera, encroaching into the Altiplano only south of 20°S. Whitman et al. (1992) suggest that the lithospheric thickness of the Altiplano decreases abruptly at about 22°S. Our cross-section at 19°30′ does not show a thick lithospheric mantle as they predict at this latitude; nevertheless a lithospheric lid is observed above an asthenospheric shallow mantle. The presence of this "cold" lithospheric lid could explain, following Whitman et al. (1992) or Kay et al. (1994) the reduction of volcanism in this region relatively to the south.

Finally, the values observed below the eastern part of the Eastern Cordillera are those found by Myers et al. (1998) ($V_p \sim 8.1$, $V_p/V_s \sim 1.76$), which are typical of subcontinental lithospheric mantle. These seismic parameters are consistent with cratonic values, and confirm the underthrusting of the Brazilian craton under the Andes. Our model indicates that the craton may be underthrusting the chain to the western limit of the Eastern Cordillera, and not just to the eastern half of the Eastern Cordillera as in Myers et al. model.

4. Conclusions

The results presented in this study lead us to propose a detailed model which allows us to explain the discrepancies between the previous models of Zandt et al. (1996) and Schmitz et al. (1997). Zandt et al. (1996) determined only a mean value of σ for the whole Altiplano. This prevents a precise description of the chain. Therefore they cannot distinguish between the Western Cordillera and the Central Altiplano Basin even when these two regions are different, as shown in Fig. 4c. Moreover they did not discuss two additional pieces of information brought by Schmitz et al. (1997). First, gravity modelling implies introduction of partially molten rocks. Second, low V_p and $\sigma = 0.25$ may indicate felsic composition but are more likely the indication of partial melt. The reasoning of Schmitz et al. (1997) is partly based on the mean value of σ determined by Zandt et al. (1996). They reject the hypothesis of felsic

composition because they consider that $\sigma = 0.25$ indicates likely partial melt. However our study shows that σ is lower than 0.25 beneath the Central Altiplano Basin. Therefore their argument seems to be valuable beneath the Western Cordillera, but is certainly not true beneath the Central Altiplano Basin.

We do not observe a low seismic anomaly extending through the lithosphere at the Altiplano/Eastern Cordillera boundary. This observation led Myers et al. (1998) to favor a process of removal of the lithosphere and replacement by asthenosphere under the largest Los Frailes volcanic field. Our V_p model shows the lower V_p zone of Los Frailes as overlaying a higher V_p zone above the CRFZ which we interpret as thick west dipping Paleozoic material. Thus the low V_p associated with Los Fariles volcanic field is without any direct relation with the low velocity anomaly observed underneath in the mantle. The presence of lamproitic magmas, spatially associated with a Quaternary shoshonitic suite, has been observed at 67°W and implies the contribution of an old cratonic lithosphere mantle in the production of recent volcanism of the Altiplano/Eastern Cordillera boundary (Carlier et al., 1996; Carlier and Lorand, 1997). Therefore, we prefer a process of in situ alteration of the lithosphere via a mechanism such as strain heating (e.g. Kincaid and Silver, 1996) to explain this volcanism.

The results of this study provide important constraints on the mechanism of the Andean orogenesis. By giving short-scale information about the crustal and upper-mantle composition, our model brings new limits on the respective involvement of crustal shortening and magmatism in the thickening of the Andean crust. Beneath the Western Cordillera, V_p and Poisson's ratio models support the idea of large areas of partially molten rocks in the lower crust above and extremely hydrated mantle down to the slab. These seismic properties are well explained by typical active volcanic arc processes and the thickening of the crust below the main volcanic arc is explained by magmatic addition. Inversely, beneath the Central Altiplano Basin and the Eastern Cordillera, our results imply thickening by compressive shortening. The close correlation observed between the main Andean faults and the boundaries of the zones with distinct seismic properties underlines their role in the crustal shortening. The seismic

properties of the Precambrian rocks outcropping indicate that their origin is in the lower crust; thus their uplift was by imbricated thrusts along westward dipping faults. The felsic composition of the lower crust beneath the Central Altiplano Basin precludes significant volume of magmatic addition, from the mantle and reinforces crustal shortening as the main thickening process. Moreover, the presence of a cratonic lower crust and of a subcontinental lithospheric upper-mantle observed under the Eastern Cordillera up to 67°W indicates the underthrusting of the Brazilian craton which is the motor of the crustal shortening. Beneath the Central Altiplano Basin, a thin lithospheric mantle is observed above a well marked asthenospheric wedge which extends in depth below the western part of the Eastern Cordillera. Thus partial melt is observed in the shallow mantle west of the Western Cordillera up to the Brazilian craton.

References

Ardill, J., Flint, S., Stanistreet, I., Chong, G., 1996. Sequence stratigraphy of the Mesozoic Domeyko Basin, northern Chile. Third ISAG St Malo, France, extended abstracts, 269–272, ORSTOM Eds, Paris, France.

Baby, P., Rochat, P., Mascle, G., Herail, G., 1997. Neogene shortening contribution to crustal thickening in the back arc of the Central Andes. Geology 25, 883–886.

Backer, M.C.W., Francis, P.W., 1978. Upper Cenozoic volcanism in the Central Andes. Ages and volumes. Earth Planet. Sci. Lett. 41, 175–187.

Basei, M., Charrier, R., Herve, F., 1996. New ages (U–Pb, Rb–Sr, K–Ar) from supposed pre-cambrian units in Northern Chile: some geotectonic implications. Third ISAG St Malo, France, extended abstracts, 763–766, ORSTOM Eds, Paris, France.

Beaumont, D., Paul, A., Beck, S., Zandt, G., 1999. Strong crustal heterogeneity in the Bolivian Altiplano as suggested by attenuation of Lg waves. J. Geophys. Res. 104, 20,287–20,305.

Carlier, G., Lorand, J.P., Bonhomme, M., Carlotto, V., 1996. A reappraisal of the Cenozoic Inner Arc Magmatism in southern Peru: consequences for the evolution of the Central Andes for the past 50 Ma. Third ISAG St Malo, France, extended abstracts, 551–554, ORSTOM Eds, Paris, France.

Carlier, G., Lorand, J.P., 1997. First occurrence of diopside sanidine phlogopite lamproites in the Andean Cordillera: the Huacancha and Morojarja dikes, southern Peru. Can. J. Earth Sci. 34 (8), 1118–1127.

Christensen, N.I., 1996. Poisson's ratio and crustal seismology. J. Geophys. Res. 101, 3139–3156.

Cunningham, P.S., Roecker, S.W., Hatzfeld, D., 1986. Three-dimensional P and S wave velocity structures of southern Peru

and their tectonic implications. J. Geophys. Res. 91, 9517–9532.

Dorbath, C., Paul, A. and the Lithoscope Andean Group, 1996. A tomography of the Andean Crust and Mantle at 20°S: first results of the Lithoscope experiment. Phys. Earth. Planet. Int. 97, 133–144.

Dorbath, C., 1997. Mapping the continuity of the Nazca Plate through its aseismic part in the Arica Elbow (Central Andes). Phys. Earth Planet. Inter. 101, 163–173.

Eberhart-Phillips, D., Michael, A.J., 1998. Seismotectonics of the Loma Prieta, California, region determined from three-dimensional V_p, V_p/V_s, and seismicity. J. Geophys. Res. 103, 21,099–21,120.

Evans, J.R., Eberhart-Philips, D., Thurber, C.H., 1994. User's manual for *simulps12* for imaging V_p and V_p/V_s: a derivative of the "Thurber" tomographic inversion *simul3* for local earthquakes and explosions. U.S.G.S., Open-file Report 94-431.

Foulger, G.R., Miller, A.D., Julian, B.R., Evans, J.R., 1995. Three-dimensional V_p and V_p/V_s structure of the Hengill Triple Junction and geothermal area, Iceland, and the repeatability of tomographic inversion. Geophys. Res. Lett. 22, 1309–1312.

Giese, P., Scheuber, E., Schilling, F., Schmitz, M., Wigger, P., 1999. Crustal thickening processes in the central Andes and the different natures of the Moho-discontinuity. J. S. Am. Earth Sci. 12, 201–220.

Graeber, F.M., Asch, G., 1999. Three-dimensional models of P wave velocity and P-to-S velocity ratio in southern central Andes by simultaneous inversion of local earthquake data. J. Geophys. Res. 104, 20,237–20,256.

James, D., 1971. Andean crustal and upper mantle structure. J. Geophys. Res. 76, 3246–3271.

Kay, S.M., Coira, B., Viramonte, J., 1994. Young mafic back arc volcanic rocks as indicators of continental lithospheric delamination beneath the Argentine Puna plateau, central Andes. J. Geophys. Res. 99, 24,323–24,339.

Kincaid, C., Silver, P., 1996. The rôle of viscous dissipation in the orogenic process. Earth Planet. Sci. Lett. 142, 271–288.

Kirby, S.H., Okal, E.A., Engdahl, E.R., 1995. The June 9, 1994, Bolivian deep earthquake: an exceptional event in an extraordinary subduction zone. Geophys. Res. Lett. 22, 2233–2236.

Kley, J., 1996. Transition from basement-involved to thin-skinned thrusting in the Cordillera Oriental of southern Bolivia. Tectonics 15, 763–775.

Kono, M., Fukao, Y., Yamamoto, A., 1989. Mountain building in the Central Andes. J. Geophys. Res. 94, 3891–3905.

Martinez, C., Soria, E., Uribe, H., 1995. Deslizamiento de cobertura en el sinclinorio mesocenozoico de Sevaruyo-Rio Mulato (Altiplano Central de Bolivia). Rev. Tec. YPFB. 16(1–2), 9–26, Cochabamba.

Masson, F., Dorbath, C., Martinez, C., Carlier, G., 2000. Local earthquake tomography of the Andes at 20°S — Implication for the structure and building of the mountain range. J. S. Am. Earth Sci. (in press).

Musacchio, G., Mooney, W.D., Luetgert, J.H., Christensen, N.I., 1997. Composition of the crust in the Grenville and Appalachian Provinces of North America inferred from V_p/V_s ratios. J. Geophys. Res. 102, 15,225–15,241.

Myers, S.C., Beck, S., Zandt, G., Wallace, T., 1998. Lithospheric-scale structure across the Bolivian Andes from tomographic images of velocity and attenuation for P and S waves. J. Geophys. Res. 103, 21 233–21 252.

Pareja, J., Vargas, C., Suarez, R., Ballon, R., Carrasco, R., Villaroel, C., 1978. Mapa geologico de Bolivia, Memoria explicativa. Serv. Geol. Bolivia/YPFB, La Paz, 27 pp.

Pinto Linconir, L., 1999. Evolucion tectonica y geomorfologica Cenozoica del borde occidental del Altiplano y su registro sedimentario entre los 19°08′–19°27′S (Region de Tarapaca, Chile). Thesis, Universidad de Chile, Santiago, 139 pp.

Riquelme, R., Hérail, G., 1997. Discordancias progresivas en el cenozoico superior del borde occidental del Altiplano de Aria: implicancias tectonicas. VIII Congreso Geologico Chileno, Antofagasta — Chile, pp. 231–235.

Rochat, P., Hérail, G., Baby, P., Mascle, G., 1999. Crustal balance and control of the erosive and sedimentary processes on the Altiplano formation. C.R.A.S.

Scheuber, E., Bogdanic, T., Jensen, A., Reutter, K.J., 1994. Tectonic development of the North Chilean Andes in relation to plate convergence and magmatism since the Jurassic. In: Reutter, K.J., Scheuber, E., Wigger, P.J. (Eds.), Tectonics of the Southern Central Andes. Springer, Berlin, pp. 121–139.

Scheuber, E., Giese, P., 1999. Architecture of the Central Andes — a compilation of geoscientific data along a transect at 21°S. J. S. Am. Earth Sci. 12, 103–107.

Schmitz, M., 1994. A balanced model of the Southern Central Andes. Tectonics 13, 484–492.

Schmitz, M., Heinsohn, W.-D., Schilling, F.R., 1997. Seismic, gravity and petrological evidence for partial melt beneath the thickened Central Andean crust (21–23°S). Tectonophysics 270, 313–326.

Sheffels, B.M., 1990. Lower bound on the amount of crustal shortening in the Central Bolivian Andes. Geology 18, 807–922.

Swenson, J.L., Beck, S.L., Zandt, G., 2000. Crustal structure of the Altiplano from broadband regional waveform modeling: implications for the composition of thick continental crust. J. Geophys. Res. 105, 607–621.

Thurber, C.H., 1983. Earthquake locations and three-dimensional crustal structure in the Coyote Lake area, central California. J. Geophys. Res. 88, 8226–8236.

Whitman, D., Isacks, B., Charelain, J.-L., Chiu, J.-M., Perez, A., 1992. Attenuation of high frequency seismic waves beneath the central Andean plateau. J. Geophys. Res. 97, 19 929–19 947.

Wigger, P., Schmitz, M., Araneda, M., Asch, G., Baldzuhn, S., Giese, P., Heinsohn, W.-D., Martinez, E., Ricaldi, E., Rower, P., Viramonte, J., 1994. Variation in the crustal structure of the southern Central Andes deduced from seismic refraction investigations. In: Reutter, K.J., Scheuber, E., Wigger, P.J. (Eds.), Tectonics of the Southern Central Andes. Springer, Berlin, pp. 23–48.

Zandt, G., Ammon, C.J., 1995. Poisson's ratio of Earth crust. Nature 374, 152–155.

Zandt, G., Beck, S.L., Ruppert, S.R., Ammon, C.J., Rock, D., Minaya, E., Wallace, T.C., Silver, P.G., 1996. Anomalous crust of the Bolivian Altiplano, Central Andes: constraints from Broadband Regional Seismic Waveforms. Geophys. Res. Lett. 23, 1159–1162.